Creep-Fatigue Interaction Effects on Pressure-Reducing Valve under Cyclic Thermo-Mechanical Loadings using Direct Cyclic Method

Nak-Kyun Cho[1*], Youngjae Choi[1], Haofeng Chen[2]

[1] Department of Manufacturing Systems and Design Engineering, Seoul National University of Science and Technology, 01811, Seoul, Republic of Korea

[2] Department of Mechanical and Aerospace Engineering, University of Strathclyde Glasgow, G1 1XJ, United Kingdom

[*]Email: nkcho@seoultech.ac.kr

Abstract

Supercritical boiler system has been widely used to increase efficiency of electricity generation in power plant industries. However, the supercritical operating condition can seriously affect structural integrity of power plant components due to high temperature that causes degradation of material properties. Pressure reducing valve is an important component being employed within a main steam line of the supercritical boiler, which occasionally thermal-fatigue failure being reported. This research has investigated creep-cyclic plastic behaviour of the pressure reducing valve under combined thermo-mechanical loading using a direct numerical method known as extended Direct Steady Cycle Analysis of the Linear Matching Method Framework (LMM eDSCA). Finite element model of the pressure-reducing valve is created based on a practical valve dimension and temperature-dependent material properties are applied for the numerical analysis. The simulation results demonstrate a critical loading component that attributes creep-fatigue failure of the valve. Parametric studies confirm the effects of magnitude of the critical loading component on creep deformation and total deformation per loading cycle. With these comprehensive numerical results, this research provides engineer with an insight into possible failure mechanisms of the pressure-reducing valve at high temperature.

Keywords: Pressure reducing valve, Creep, Cyclic plasticity, The linear matching method, Supercritical boiler

1. Introduction

Conventional power plants generate electricity with turbines powered by hot steam generated from boiler system. After centuries of development, a supercritical boiler system was developed and now frequently used at commercial power plants, since it can generate the electricity more efficiently with superheated steam [1]. One of crucial parts of a supercritical boiler system is a pressure-reducing valve (PRV) that places at the main-steam pipe line, and reduces high temperature and pressure of the superheated steam before it flows into start-up vessel (SUV). Considering the harsh operating condition of PRV, it requires to be designed securing a high level of safety against potential accidents such as crack initiation caused by creep-fatigue damage.

For such components subjected to complex cyclic loading at the high temperature, it is hard to predict structural behaviours that involves inelastic strains accumulated in combination of creep and plastic deformation over every cyclic loading. In addition, two typical phenomenon, creep and stress relaxation, observed from materials at high temperature can have significant impacts on the structural integrity with creep-fatigue interaction [2, 3]. Industry standards such as R5 procedures[4], ASME NH code [5], and RCC-MRx [6] are commonly used in safety cases for structural integrity assessment of high temperature component. However theses rule based methods predict overly conservative structural behaviours, leading to short life expectancy. Moreover it is not eligible for a structure exhibiting complicated stress-strain behaviours. For such cases, the standards also recommend to conduct detailed structural integrity assessment of high temperature component considering temperature dependent material behaviours using inelastic finite element (FE) analysis.

FE based analysis have been developed and improved greatly, especially direct methods have demonstrated that it can balance between time-efficiency and accuracy compared to the time-consuming step by step analysis. One of well-known direct methods is the Linear Matching Method Framework (LMMF) that analyse cyclic plastic behaviour such as shakedown and ratchetting [7, 8]. The LMMF also include an augmented numerical procedure called extended Direct Stress Cycle Analysis (eDSCA) that can analyse cyclic structural response considering creep-fatigue interaction [9]. Recently, application of eDSCA has been extended to predicting creep-fatigue interaction with temperature

dependent creep properties and capable of calculating creep-fatigue damage using different damage models [10]. Over the last decade, the LMMF have been utilised to analyse complicated structural problems that involve, especially, high temperature [11-13]. Hence, this research has conducted to evaluate structural behaviour of PRV with the modified eDSCA method.

Cho et al. presented a cyclic plastic behaviour of the PRV under cyclic thermo-mechanical loading but creep effects was not considered [14]. The objective of this research is to analyse the creep cyclic plasticity behaviour of the PRV subjected to complex cyclic thermo-mechanical loadings that comprised of cyclic system moments (in-plane, out-of-plane, and torsion), cyclic internal pressure, and cyclic thermal loads. The effect of individual system moment and of combined system moment level on both creep and plastic deformation are investigated. Numerical results exhibit factors to affect those structural integrity of the PRV and causes are discussed. Based on findings, this research provides insight into possible failure mechanism of the PRV at high temperature.

This paper structures as follows. Section 2 describes numerical procedures of the LMM eDSCA. Section 3 provides the problem descriptions of this research such as finite element model created for the analysis, material properties used and parameters considered for this numerical analysis. The numerical results and discussions are presented in the Section 4. Finally, Section 5 concludes this research.

2. **Direct Steady Cycle Analysis Method**

Creep cyclic plastic behaviour of the pressure-reducing valve is assessed using an extended Direct Steady Cycle Analysis (eDSCA) method of The Linear Matching Method Framework [9]. The eDSCA procedure calculates the cyclic stress history at the steady cycle state in associated with residual stresses accumulated by inelastic strains either plastic or creep during the loading cycle. The eDSCA utilise a minimization procedure that has an assumption that plastic strain only occurs at time t_n, where N (from n = 1 to N) denotes total number of loading instances. The minimization function of the eDSCA in an incremental form can be given by Eq.(1).

$$I^n\left(\Delta\varepsilon_{ij}^n\right) = \int_V \left\{\sigma_{ij}^n \Delta\varepsilon_{ij}^n - \left[\hat{\sigma}_{ij}(t_n) + \rho_{ij}^r(t_n)\right]\Delta\varepsilon_{ij}^n\right\} dV \geq 0 \qquad (1)$$

By an iterative process, the strain increment $\Delta\varepsilon_{ij}^{n}$ can be calculated by the minimization process until the requested a total number of cycles *M*. The number of load instances *N* is performed as sub-cycles within each cycle *m*, where *m* (from *m* = 1 to *M*). Hence, the accumulated residual stress for n^{th} load instance at m^{th} cycle of iterations can be expressed by Eq.(2).

$$\rho_{ij}^{r}(t_n)_m = \sum_{i=1}^{m-1}\sum_{n=1}^{N}\Delta\rho_{ij}^{r}(t_n)_i + \sum_{i=1}^{n}\Delta\rho_{ij}^{r}(t_i)_m \quad (2)$$

For example, if the cycles *m* and *m*+1 are only considered, the iterative shear modulus $\bar{\mu}_n(t_n)$ at a load instance t_n can be defined by Eq.(3), where $\sigma_y(t_n)_m$ denotes the von-Mises yield stress of the elastic perfectly plastic model, which is substituted to creep flow stress $\bar{\sigma}_c$ when the $t_n$involves a load instance of creep.

$$\bar{\mu}_{m+1}(t_n) = \bar{\mu}_m(t_n)\frac{\sigma_y(t_n)_m}{\bar{\sigma}(\hat{\sigma}_{ij}(t_n)+\rho_{ij}^{r}(t_n)_m} \quad (3)$$

Without consideration of a load instance of creep, the inelastic strain increment $\Delta\varepsilon_{ij}^{n}(t_n)_{m+1}$ at the cycle *m*+1 can be calculated by Eq.(4), where $\rho_{ij}^{r}(t_{n-1})$ is the accumulated previous residual stress before the time t_n and the notation (') refers to the deviatoric component:

$$\Delta\varepsilon_{ij}(t_n)'_{m+1} = \frac{1}{2\bar{\mu}_m(t_n)}\left\{\hat{\sigma}_{ij}(t_n) + \Delta\rho_{ij}^{r}(t_{n-1})_{m+1} + \Delta\rho_{ij}^{r}(t_n)_{m+1}\right\}' \quad (4)$$

where the residual stress accumulated at the cycle *m* is the summation of the previous varying residual stress and constant residual stress.

$$\rho_{ij}^{r}(t_{n-1})_m = \rho_{ij}^{r}(t_0) + \Delta\rho_{ij}^{r}(t_1) + \Delta\rho_{ij}^{r}(t_2) + \cdots + \Delta\rho_{ij}^{r}(t_{n-1}) \quad (5)$$

To calculate creep strain accumulated during a dwell period, time hardening power law shown in Eq. (6) is used to calculate creep deformation, where $\dot{\bar{\varepsilon}}^{c}$ is the effective creep strain rate; $\bar{\sigma}$ is the von-Mises stress, t is the dwell time; A, *n* and *m* are creep constants.

$$\dot{\bar{\varepsilon}}^{c} = A \cdot \bar{\sigma}^{n} \cdot t^{m} \quad (6)$$

It is assumed that the stress relaxation process follows a linear relation that has been generally defined as Eq. (7) with an elastic follow-up factor Z, where $\bar{E}$ is the effective modulus of elasticity which can be defined as $\bar{E} = 3\mathrm{E}/2(1+\upsilon)$; E is the modulus of elasticity; υ is the Poisson's ratio; $\dot{\bar{\sigma}} = \dot{\bar{\sigma}}(\sigma_{ij})$.

$$\dot{\bar{\varepsilon}}^c = -\frac{Z}{E}\dot{\bar{\sigma}} \tag{7}$$

Eq. (6) and Eq. (7) are combined and then integrated the combined equation over the dwell time Δt:

$$\frac{A\bar{E}\Delta t^{m+1}}{Z(m+1)} = \frac{1}{n-1}\left(\frac{1}{\bar{\sigma}_c^{-n+1}} - \frac{1}{\bar{\sigma}_s^{-n+1}}\right) \tag{8}$$

where $\bar{\sigma}_s$ is the start of the dwell stress; $\bar{\sigma}_c$ is the end of the dwell stress (creep flow stress) which replace the $\sigma_y(t_n)_m$ in Eq.(3) within the iterative process. Integrating Eq. (7) over the dwell time Δt and then combined with Eq.(8) in order to eliminate $Z/\bar{E}$, where $\Delta\bar{\varepsilon}^c$ is the effective creep strain increment over the dwell time.

$$\Delta\bar{\varepsilon}^c = \frac{A(n-1)\Delta t^{m+1}(\bar{\sigma}_s - \bar{\sigma}_c)}{(\bar{\sigma}_c^{-n+1} - \bar{\sigma}_s^{-n+1})(m+1)} \tag{9}$$

The creep strain rate $\dot{\bar{\varepsilon}}^c$ at the end of the dwell time Δt is calculated from Eq.(8) and Eq.(9).

$$\dot{\bar{\varepsilon}}^c = \frac{\Delta\bar{\varepsilon}^c(m+1)\bar{\sigma}_c^n}{(n-1)(\bar{\sigma}_s - \bar{\sigma}_c)\Delta t}\left(\bar{\sigma}_c^{-n+1} - \bar{\sigma}_s^{-n+1}\right) \tag{10}$$

Initially the iterative process starts with estimated $\bar{\sigma}_s$ and $\bar{\sigma}_c$ values and the Eq.(9) and Eq.(10) compute new creep flow stress $\bar{\sigma}_c^f$ using Eq.(11), so that the $\bar{\sigma}_c^f$ replace $\sigma_y(t_n)_m$ in Eq.(3) to carry out the linear matching condition.

$$\bar{\sigma}_c^f = \left(\frac{\dot{\bar{\varepsilon}}^c}{A\Delta t^m}\right)^{\frac{1}{n}} \tag{11}$$

3. **Problem Descriptions**

3.1. Finite element model

The pressure-reducing valve is comprised of a valve body, four welded pipes, and a thermal seal that is placed inside of the valve. Dimensions and half geometry view of the pressure-reducing valve are shown in Table 1 and Figure 1 respectively. The thermal seal was modelled for heat transfer analysis but

removed for the creep cyclic plastic analysis since vulnerable locations against the thermo-mechanical loadings are the valve body rather than the seal, according to simulation results.

Table 1. Pressure-reducing valve dimensions (mm).

	Outer radius	Inner radius	r/t ratio
Branch Pipe	96.0	60.0	2.2
Flange Pipe	158.2	91.9	1.9
Warming Line	40.0	25.0	2.2
Main Pipe	100.0	74.0	3.4

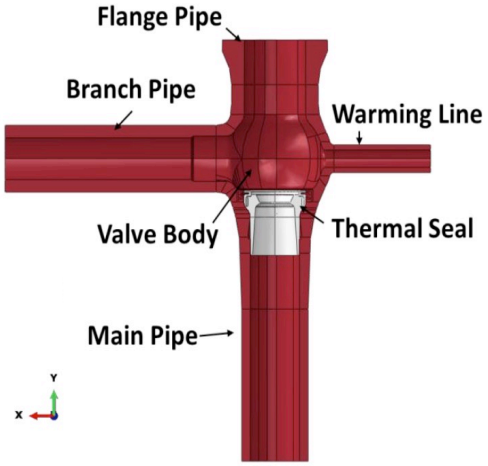

Figure 1. The half geometry of the pressure-reducing valve

3D solid element type, C3D8R, has been used to mesh the pressure-reducing valve in Abaqus (version 6.12-3) and a fully meshed model is presented in Figure 2. Mesh sensitivity studies were carried out by comparing equivalent stress with a model meshed with an element type of C3D20R, which results confirm deviation of the stress magnitude less than 3%.

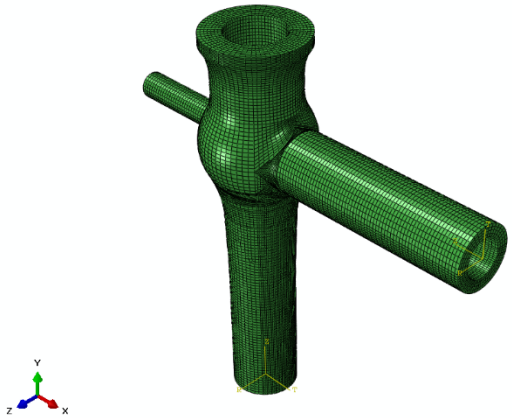

Figure 2. Fully meshed model with 3D solid elements.

For boundary condition, a reference node is created at bottom centre of the main pipe and kinematic coupling is applied between the reference node and bottom surface of the main pipe, which allows displacement in a radial direction of the main pipe but rest directions are fully constrained.

3.2. Material properties

The pressure-reducing valve is made of Type 316 stainless steel. Physical properties and yield strength of the material are assumed to be the same as the previous research [14]. To simulate more realistic structural behaviour, temperature dependent material properties are employed. The material properties applied for the finite element model is summarised in Table 2. For non-linear behaviour, elastic perfectly plastic model is considered.

Table 2. Temperature dependent physical properties and yield strength of Type 316 stainless steel.

Temp.[°C]	E [MPa]	υ	σ_y [MPa]
20	198298	0.29	179.48
100	192290		148.68
200	184780		122.32
300	177270		106.36
400	169760		97.52
500	162250		92.51
550	158495		90.42

For temperature related material properties, transient heat transfer model is developed with temperature dependent thermal conductivity and film coefficient for the start-up period of 36000 seconds, equivalent to 10hours, which analysis result is shown in Figure 4. For predicting creep behaviour, creep deformation model with power law is employed as Eq. (12) and Arrhenius law is used to implement temperature dependent creep deformation as Eq. (13)

$$\dot{\varepsilon}_{creep} = A^* t^m \sigma^n \tag{12}$$

$$A^* = A \cdot exp\left(^{-Q}/_{RT}\right) \tag{13}$$

,where A^*, m, n are the creep parameters; t is the dwell time; σ is the equivalent dwell stress; A is material constant; Q is the activation energy; R is the gas constant; T is the absolute temperature [K]. Parameters related to the temperature dependent creep deformation are summarised in Table 3.

Table 3 Material properties for temperature dependent creep deformation for Type 316 stainless steel.

Parameter	Value	Temp.[°C]
m	-0.587	540
n	4.1578	540
A	1.509 x 10^8	n/a
Q [J]	314000	540
R [$J \bullet mol^{-1} \bullet K^{-1}$]	8.31	n/a

3.3. Cyclic thermo-mechanical loadings

The pressure-reducing valve has experienced following cyclic thermo-mechanical loadings: system moments, internal pressures, and thermal loads. The system moment has come from pipelines connected before the branch pipe. The system moment consist of in-plane bending, out-of-plane bending, and torsional moment. Figure 3 presents the applied system moments and pressures. To implement the system moment, a reference node is created at centre of the branch pipe end and kinematic coupling is connected between the node and the branch pipe end surface, which allows radial expansion only. Referenced system moments and torsion are calculated from Eq. (14) and Eq. (15)

$$M_0 = \frac{4}{3}\sigma_y(R_0^3 - R_i^3) \tag{14}$$

$$T_r = \tau_{max} \cdot \frac{J_T}{r_{mean}} \tag{15}$$

, where M_0 is the limit bending moment of thick walled pipe; σ_y is the yield strength of the material; R_0 and R_i are the radius of the thick walled pipe respectively; T_r is the limit torque; τ_{max} is the maximum shear strength of the material; J_T is the torsion constant for the section; r_{mean} is the mean radius of the pipe section.

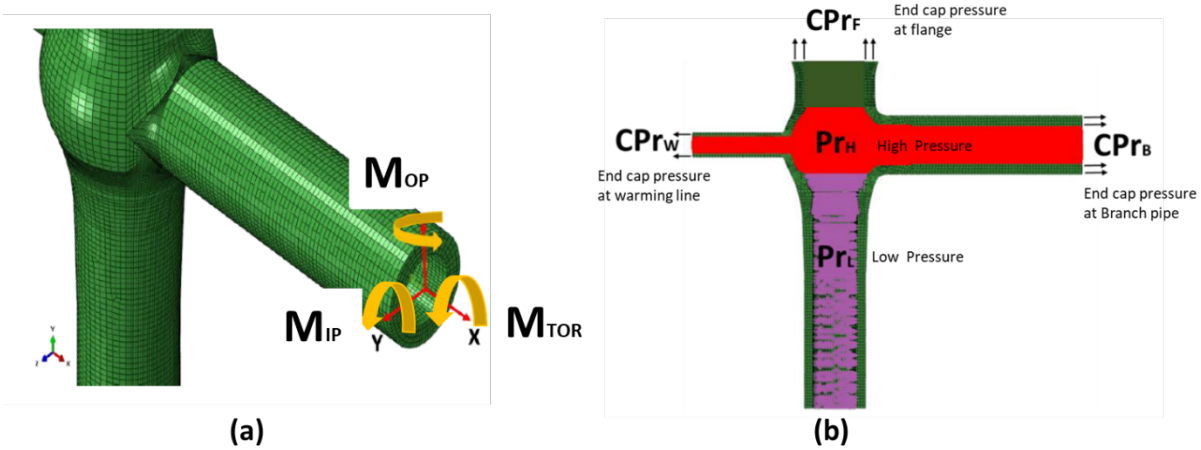

Figure 3. Applied mechanical loadings: (a) bending and torsional moments at branch pipe and (b) internal pressures and end cap pressures.

Internal pressures taking place during the start-up period are taken for normal operating condition of a supercritical boiler system. Figure 3 (b) presents the inside of the pressure-reducing valve locations where the pressurised steam applied. All pipe ends are assumed as closed-end condition, which results in end-cap pressure acting on all pipe ends subjected to high pressure. End-cap pressure at the flange pipe has considered the effect of the end-cap pressure at the main pipe. The end-cap pressures are calculated from Eq. (16).

$$\sigma_l = \frac{p_i r_i^2 - p_o r_o^2}{r_o^2 - r_i^2} \tag{16}$$

, where σ_l is the end-cap pressure; p_i and p_o are internal pressure and external pressure of the thick walled pipeline respectively; r_i and r_o are the inside radius and outside radius of the thick walled pipeline respectively. The calculated system moments and pressures are summarised in Table 4

Table 4 Applied pressure loading and system moment loadings

Loading	Pressure[MPa]	Loading	Moments[Nmm]
Pr_H	19.10	M_{IP}	8.06 x 10^7
Pr_L	5.31	M_{OP}	8.06 x 10^7
CPr_F	3.31	M_{TOR}	8.52 x 10^7
CPr_B	12.24		
CPr_W	12.24		

Thermal loading is obtained by a transient heat analysis as shown in Figure 4. Initial temperature is assumed as room temperature of 20 degree Celsius. During the start-up period, the maximum temperature reaches up to 550 degree Celsius over high pressurised steam path line from the branch pipe to warming line. When the pressure –reducing valve activates, high pressurised steam with high temperature cool down by water spray inside of the valve body and the temperature and pressure are lowered to 350 degree Celsius and 5.3 MPa respectively and going into the start-up vessel through the main pipe.

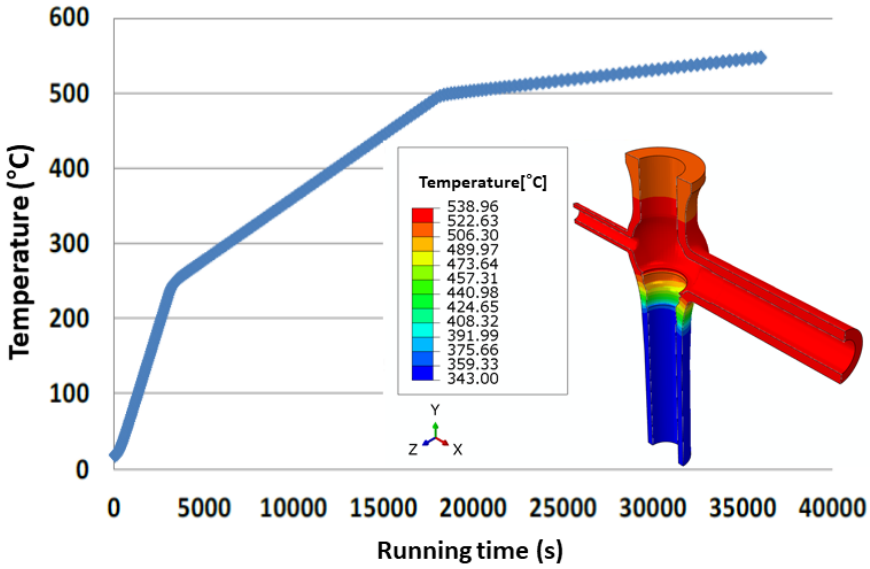

Figure 4. Heat-transfer analysis results and temperature gradient of the pressure-reducing valve for start-up period, 10hours.

Loading cyclic is designed as Figure 5. In creep cyclic plastic analysis, both the referenced pressure loading and thermal loading are applied as from 0.0 to 1.0, which are the normalised value. To evaluate the effect of individual system moment, each system moment with normalised value of 1.0 is applied together with the thermal and pressure loadings. In addition, the effect of the system moment on the structural integrity of the pressure-reducing valve is assessed for changes in the system moment from normalised value of 0.1 to of 0.4 with the pressure and thermal loadings.

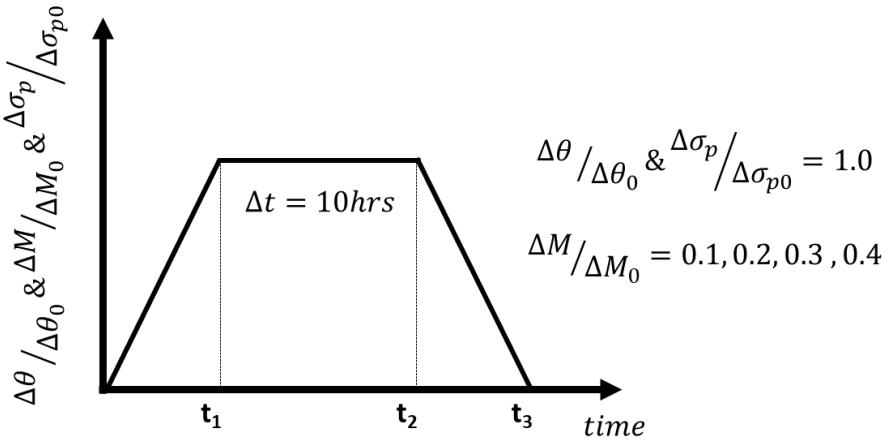

Figure 5. Applied loading waveform under loading (t_1)-dwell (t_2)-unloading (t_3) cyclic loading for start-up period, 10hours.

4. Numerical results and discussions

4.1. Linear elastic and cyclic plastic behaviour

Linear elastic behaviour and cyclic plastic behaviour of the pressure-reducing valve under the same thermo-mechanical loading were presented by a previous study [14]. As it can be seen in Figure 6, inside crotch corner of the pressure-reducing valve develops the maximum equivalent stress against the pressure and thermal loading. Whereas the system moment induces the maximum equivalent stress at outside of weldment connected between the branch pipe and valve body. For all thermo-mechanical loading applied, the maximum equivalent stress takes place at lower weldment zone of the branch pipe to the valve body.

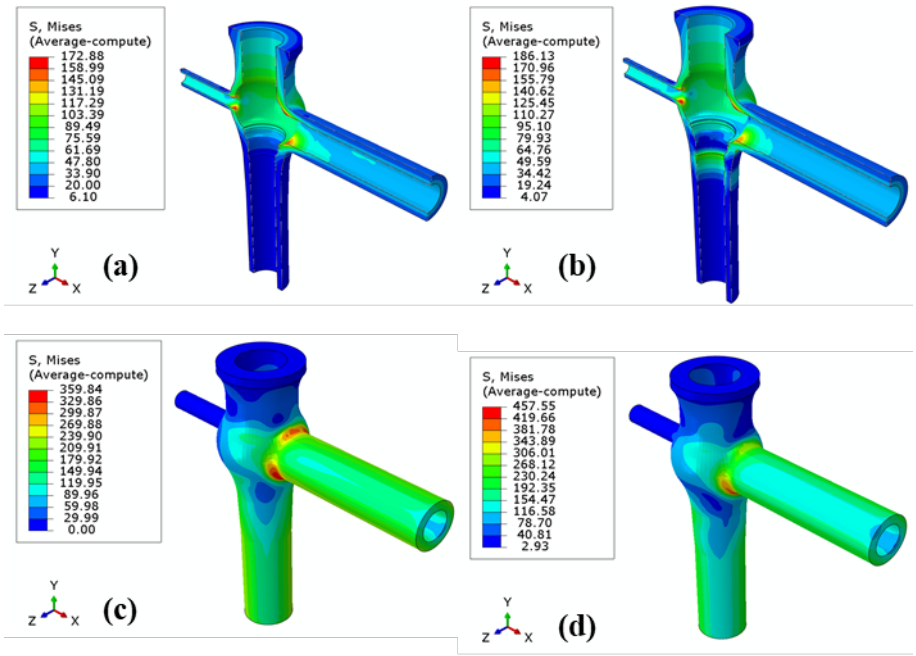

Figure 6. Elastic behaviour of the pressure-reducing valve against applied loadings: (a) internal pressure only, (b) internal pressure and thermal loading, (C) system moment loading only, and (d) all thermo-mechanical loadings.

The previous study also showed cyclic plastic analysis of the pressure-reducing valve against the thermos-mechanical loading and revealed an elastic shakedown boundary is identical to a plastic collapse limit, since primary stress dominate the developed equivalent stress. As shown the plastic

collapse limit in Figure 7, when the pressure-reducing valve is subjected to normalised cyclic thermal and pressure value of 1.0, the maximum normalised cyclic system moment must be less than 0.45, otherwise plastic collapse will occur. Hence, the effect of the system moment on creep-cyclic plastic behaviour is assessed for the normalised system moment up to 0.4.

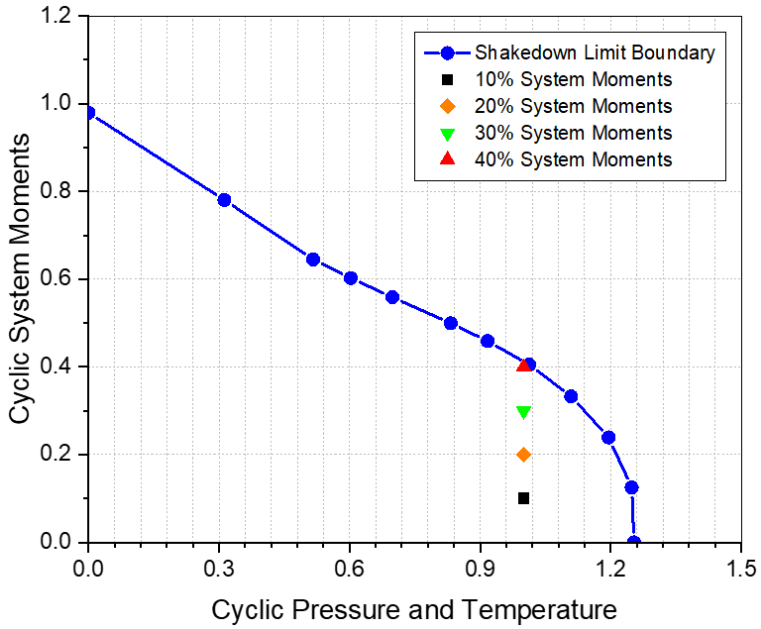

Figure 7. Elastic shakedown limit boundary of the pressure reducing valve against the cyclic thermo-mechanical loading.

4.2. Creep cyclic plastic behaviour

In order to evaluate effects of an individual system moment on structural integrity of the pressure-reducing valve, creep cyclic plastic analysis is carried out against cyclic moment with normalised value of 0.3 for a dwell time of 10 hours. Figure 8 shows creep deformation contours against the individual moment effect. Critical locations with creep deformation are observed from inside upper crotch corner of warming line, inside upper crotch corner of branch pipe, and outside weldment of branch pipe against in-plane, out-of-plane, and torsional moment respectively.

It can be seen from the simulation results that significant creep deformation does not develop per cycle. Creep deformation per cycle is larger in order of out-of-plane moment, in-plane moment, and torsional moment. Maximum total deformation occurs at the same location as the maximum creep deformation

takes place and larger in order of in-plane moment, torsional moment, and out-of-plane moment. Table 5 presents summarised equivalent stress history, creep deformation and total deformation per cycle.

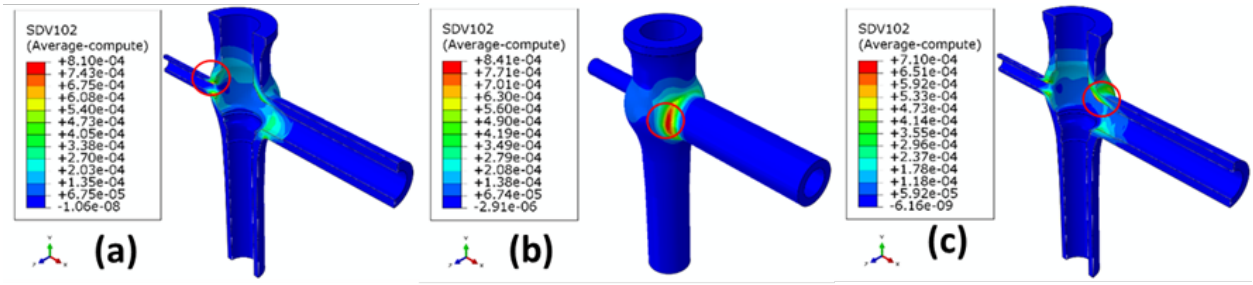

Figure 8 Absolute creep strain per cycle with temperature dependent creep effects against cyclic system moment normalised as 0.3: (a) in-plane, (b) out-of-plane, and (c) torsional.

As it can be seen from Table 5, no yielding occurs at both loading and unloading periods, resulting in no plastic deformation developed except the inelastic creep deformation over a cycle. Figure 9 depicts stress-strain hysteresis loop of the critical location with creep deformation against the individual system moment loading.

Table 5 Equivalent stress history and creep deformation per cycle of the critical location, and total deformation per cycle against individual system moment case.

System moment	Loading [MPa]	Creep [MPa]	Unloading [MPa]	Creep strain [abs]	Total strain [abs]
In-Plane	87.97	88.66	-103.5	8.10E-04	1.82E-03
Out-of-Plane	89.37	89.72	-54.87	8.41E-04	1.74E-03
Torsional	85.65	85.66	-82.65	7.10E-04	1.76E-03

It is worth mentioning that there is no apparent stress relaxation during a dwell period. This type of relaxation can take place when the primary stress has more effects on the PRV than the secondary stress. For instance, let's assume that both primary stress in tension and secondary stress in compression are imposed on the PRV under thermo-mechanical loading. Combined equivalent stress level at loading instance can be reduced by the secondary stress. However the compressive secondary stress begins to

relax at creep instance, which leads to the primary stress in tension affects more to equivalent stress. The increase in dwell stress is a possible high temperature mechanism when rupture reference stress is higher than start of dwell stress, and they are introduced in R5 procedures [15] and other researches [10, 16].

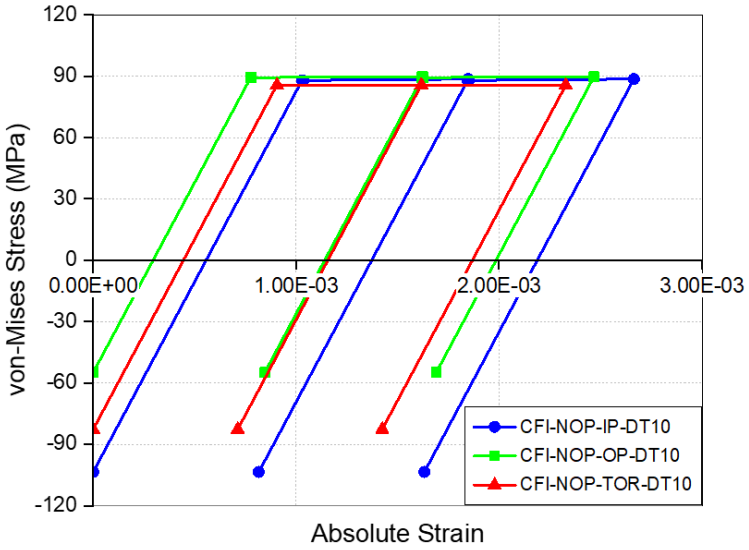

Figure 9 Stress-strain hysteresis loop of critical location with creep deformation against individual system moments.

To evaluate the effects of the temperature dependent creep parameters on the creep-cyclic plasticity, structural response of the PRV is analysed against the same cyclic system moment using the original LMM eDSCA that employees a temperature independent creep parameters (A = 2.70E-12; n=4.1578; m=-0.587, at 540°C).

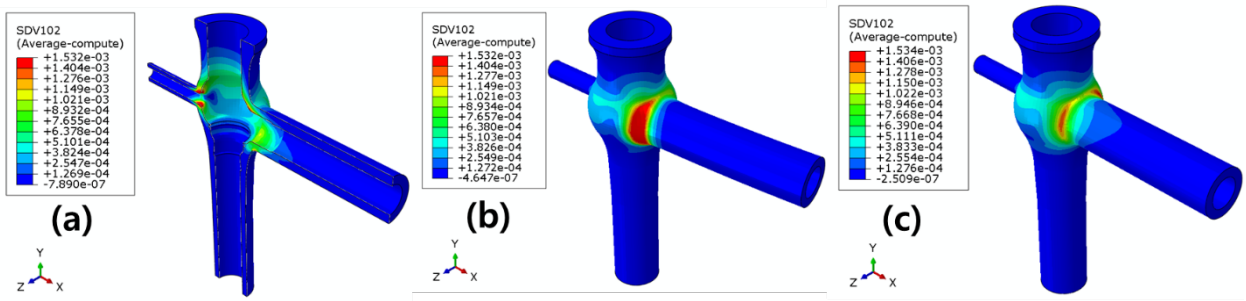

Figure 10 Absolute creep strain per cycle with temperature independent creep effects against cyclic system moment normalised as 0.3 : (a) in-plane, (b) out-of-plane, and (c) torsional.

Figure 10 depicts the overall creep deformation of the PRV with the effect of the temperature independent creep parameters against the individual cyclic system moments. The maximum creep strain occurs at the identical location to individual system moment effects shown in Figure 8 but the amount of the deformation almost doubled. As can be seen in Figure 4 the PRV has temperature gradient along with vertical direction not with through thickness, so that resultant thermal stress as Figure 6 (b) is developed over the connecting area between main pipe and valve body and flange pipe and valve body. Owing to the independent creep parameters it can be presumed that the PRV may experience exaggerated creep deformation with the relatively lower temperature area such as the connecting zone with the valve body, affecting to structural integrity of the PRV.

Another creep-cyclic plastic analysis is conducted to evaluate the effects of combined system moment level on structural integrity of the pressure-reducing valve. The level of the combined system moment increases from normalised value of 0.1 to 0.4 and the dwell time of 10 hours is considered. Figure 11 presents creep deformation contour per cycle against the effects of combined system moment level. Maximum creep deformation take place at inside upper crotch corner of the warming line against the normalised combined system moment level up to 0.2 but it shifts to outside and then inside weldment of the branch pipe when the level reaches 0.3 and 0.4 respectively. Table 6 summarises the equivalent stress history and creep deformation per cycle of the critical location, and maximum total deformation per cycle taken from the pressure-reducing valve.

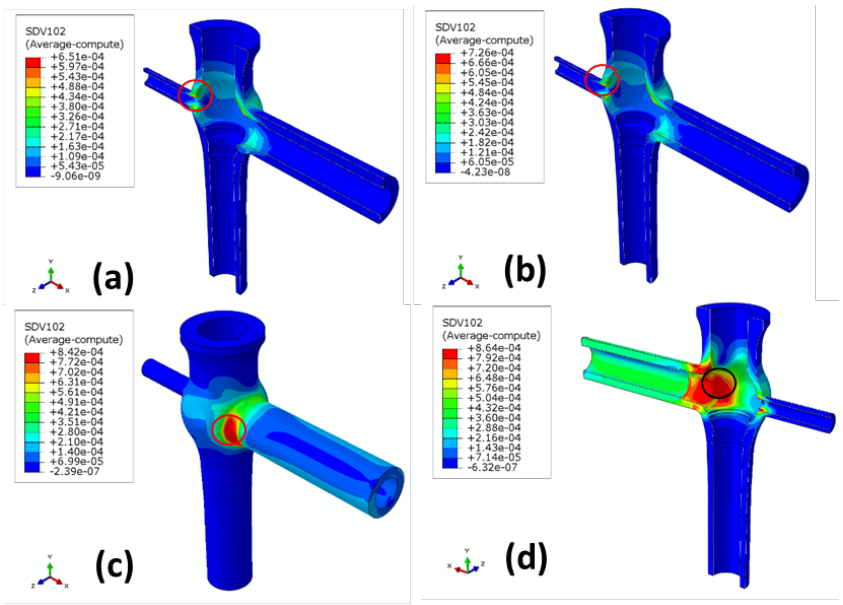

Figure 11 Creep deformation per cyclic against the combined system moment level: (a) 10%, (b) 20%, (c) 30%, and (d) 40%.

The maximum total deformation takes place at the same location as the maximum creep deformation occurs when the moment level raise up to 0.2 but at different locations when the moment level is greater than 0.2. As can be seen from Table 6 the effect of the combined moment level on creep deformation per cycle is not substantial but significant impacts to total strain accumulation per cycle. This is because the pressure-reducing valve experiences yielding when subjected to the combined moment level over 0.3, which results in more than twice total strain accumulated at the moment level of 0.4 than of 0.3.

Table 6 Equivalent stress history and creep deformation per cycle of the critical location, and total deformation per cycle against normalised combined system moment.

Combined moment	Loading [MPa]	Creep [MPa]	Unloading [MPa]	Creep strain [abs]	Total strain [abs]
10%	84.46	85.19	-93.9	6.51E-04	1.80E-03
20%	84.72	87.34	-98.32	7.26E-04	1.92E-03
30%	87.75	91.63	-45.08	8.42E-04	2.22E-03
40%	88.26	91.63	-18.51	8.64E-04	5.12E-03

Figure 12 illustrates stress-strain hysteresis loops of critical locations against each moment level. As the same trend as the individual moment effects showed, primary stress dominates overall stress of the critical locations, resulting in stress relaxation not taking place during a dwell period. Moreover, as moment level increases, the critical locations tend to have larger creep deformation per cycle but smaller total deformation per cycle due to decrease in unloading stress level.

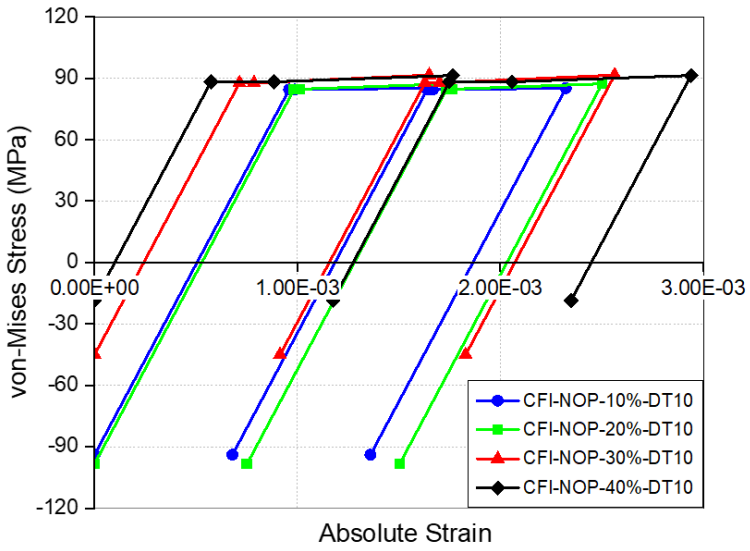

Figure 12 Stress-strain hysteresis loop of critical location with creep deformation against combined system moments.

Overall, it is found out that out-of-plane moment develops the largest creep deformation per cycle among the three concerned system moments but amount of the creep deformation per cycle does not affect critically to structural integrity of the pressure-reducing valve under the given loading condition. In additions, as the moment level increases, the pressure-reducing valve experiences plastic deformation more than creep deformation. Hence it is predicted that fatigue failure is likely to occur rather than creep related failure at higher moment level.

5. Conclusions

Creep cyclic plastic analysis of the pressure-reducing valve was conducted against cyclic thermal load, cyclic internal pressure, and cyclic system moments (in-plane, out-of-plane, torsional) using the Linear Matching Method eDSCA. The effects of individual system moment and combined system moment level on structural integrity of the pressure-reducing valve were assessed and following numerical results have been obtained.

For the effect of the individual system moments, out-of-plane moment revealed the largest creep strain accumulated per cycle, but each moment developed a more or less the same total deformation per cycle. There was interesting point observed that no apparent stress relaxation occurred during a dwell period due to dwell stress dominated by primary stress. As shown stress-strain hysteresis loops per cycle in Figure 9, it can be predicted that the structural integrity of the pressure-reducing valve may be threaten with the system moments, leading to creep enhanced ratchetting response. A comparative study on the effects of temperature dependents creep parameters revealed that structural integrity assessment with independent creep parameter predict more conservative creep deformation per cycle. Further parametric study was performed to evaluate the effect of the moment level on the structural integrity of the valve and presented that total deformation is attributed to plastic deformation more than creep deformation per cycle as the moment level increase. Hence it can be presumed that the pressure reducing valve is likely to experience crack due to fatigue damage rather than creep damage, when significant system moment is applied during operation.

This research presented potential high temperature failure mechanism of the pressure reducing valve that is generally attached in the main steam line of supercritical boiler system. Assessment results demonstrated the effect of system moments on the integrity of the pressure reducing valve, which provide design engineer with insight into creep-cyclic plasticity of the valve under the complex loading. Moreover, this research showed the Direct Steady Cycle Analysis method can be an efficient analysis manner for detailed inelastic structural analysis.

Acknowledgement

This study was supported by the Research Program funded by the SeoulTech (Seoul National University of Science and Technology). Authors would like to gratefully acknowledge supports from ***Engineering Analysis Services Limited UK*** during the course of this work.

References

1. Abe, F., *Progress in Creep-Resistant Steels for High Efficiency Coal-Fired Power Plants.* Journal of Pressure Vessel Technology, 2016. **138**(4).
2. Cho, N.-K., et al., *Enhanced fatigue damage under cyclic thermo-mechanical loading at high temperature by structural creep recovery mechanism.* International Journal of Fatigue, 2018. **113**: p. 149-159.
3. Giugliano, D., et al., *Creep-fatigue and cyclically enhanced creep mechanisms in aluminium based metal matrix composites.* European Journal of Mechanics - A/Solids, 2019. **74**: p. 66-80.
4. Ainsworth, R., British Energy Generation Ltd, *R5: Assessment procedure for the high temperature response of structures.* 2003. **3**.
5. ASME III, B. *Section III-Rules for Construction of Nuclear Facility Components-Division 2-Code for Concrete Containments*. 2015. ASME.
6. RCC-MRx, A., *Code of Design and Construction Rules for Mechanical Component in Nuclear Installations*. 2013.
7. Chen, H., et al., *The linear matching method applied to the high temperature life integrity of structures. Part 1. Assessments involving constant residual stress fields.* International Journal of Pressure Vessels and Piping, 2006. **83**(2): p. 123-135.
8. Chen, H. and A. Ponter, *Integrity assessment of a 3D tubeplate using the linear matching method. Part 1. Shakedown, reverse plasticity and ratchetting.* International Journal of Pressure Vessels and Piping, 2005. **82**(2): p. 85-94.
9. Chen, H. and A. Ponter, *Linear Matching Method on the evaluation of plastic and creep behaviours for bodies subjected to cyclic thermal and mechanical loading.* International Journal for Numerical Methods in Engineering, 2006. **68**(1): p. 13-32.
10. Cho, N.-K., et al., *Creep-fatigue endurance of a superheater tube plate under non-isothermal loading and multi-dwell condition.* International Journal of Mechanical Sciences, 2019. **161-162**: p. 105048.
11. Cho, N.-K., et al., *Investigating the Effects of Cyclic Thermo-Mechanical Loading on Cyclic Plastic Behavior of a Ninety-Degree Back-to-Back Pipe Bend System.* Journal of Pressure Vessel Technology, 2019. **142**(2).
12. Zheng, X., et al., *A novel fatigue assessment approach by Direct Steady Cycle Analysis (DSCA) considering the temperature-dependent strain hardening effect.* International Journal of Pressure Vessels and Piping, 2019. **170**: p. 66-72.
13. Ma, Z., et al., *A direct approach to the evaluation of structural shakedown limit considering limited kinematic hardening and non-isothermal effect.* European Journal of Mechanics - A/Solids, 2020. **79**: p. 103877.
14. N. Cho, P.B., A. M. Hurst, *Investigating structural response of pressure reducing valve of supercritical steam generator system under cyclic moments, thermal transient, and pressure loadings*, in *Proceedings of the 28th International Conference on Nuclear Engineering*. 2020, ASME: Anaheim, California, USA.

15. Ainsworth, R., P. Budden, and R. Hales, *Assessment of the high-temperature response of structures: developments in the R5 procedure*, in *Creep and fatigue. Design and life assessment at high temperature. Proceedings*. 1996.
16. Giugliano, D., et al., *Cyclic plasticity and creep-cyclic plasticity behaviours of the SiC/Ti-6242 particulate reinforced titanium matrix composites under thermo-mechanical loadings.* Composite Structures, 2019. **218**: p. 204-216.